Journal of Applied Fluid Mechanics, Vol. 15, No. 6, pp. 1801-1813, 2022.
Available online at www.jafmonline.net, ISSN 1735-3572, EISSN 1735-3645.
https://doi.org/10.47176/jafm.15.06.1236

Investigations on the Interfering Factor of Single Synthetic Jet Actuator on Improving the Efficiency of Wing Control Surface

Y. Zhou[1,2], S. Zheng[3] and J. Chang[1,2†]

[1] *College of Mechatronic Engineering, North University of China, Taiyuan 030051, China*
[2] *Institute of Military-Civilian Integration and Innovation, North University of China, Taiyuan 030051, China*
[3] *State owned Changhong Machinery Factory, Guilin 541002, China*

†*Corresponding Author Email: changjl@nuc.edu.cn*

(Received April 17, 2022; accepted July 19, 2022)

ABSTRACT

After the deflection of the wing control surface, flow separation is easily generated at the trailing edge of the wing, which will reduce the lift coefficient and the control surface efficiency. The rudder of the wing is aileron. If the lift generated by the wing is used to improve the efficiency of the control surface, the flow separation caused by the deflection of the control surface must be restrained. Using synthetic jet to change the flow state of boundary layer is the main method to solve the problem of flow separation. Synthetic jet actuator (SJA) has the advantages of no energy loss and simple structure. In this paper, a method of using synthetic jet actuator to suppress the flow separation at the rear of the wing when the aileron deflects is proposed, and the lift coefficient is obtained. The increase of aileron efficiency is calculated by the change of lift coefficient. The EPPLER555 wing with aileron deflection angle of 3°~9° is simulated, and the changes of lift coefficient and aileron efficiency under corresponding working conditions are obtained. The results show that the average lift coefficient of the wing is 0.5 when the deflection angle of the aileron is 3°~9° without SJA. After SJA employed, the lift coefficient will be greatly improved, and the control surface efficiency of EPPLER555 wing will be effectively improved, the lift coefficient will increase by about 20% to 0.6-0.7. For example, when the deflection angle of aileron is 4°, using a SJA with a maximum outlet velocity of 200m/s and an excitation frequency of 400/2π, the effective lift coefficient generated by the wing is 0.5931. Under the effect of SJA, the control surface efficiency of EPPLER555 wing will be effectively improved. The lift coefficient is reflected by the ratio of the change of lift coefficient after SJA employed to the lift coefficient without synthetic jet actuator.

Keywords: Single synthetic jet actuator; Wing control surface; Interfering factor; EPPLER555; Lift coefficient.

NOMENCLATURE

Cl_{eff}	effective value of lift coefficient	Cl_a	when the aileron is deflected by a certain angle, but the synthetic jet exciter is not working, the lift coefficient of the wing
$L(t)$	lift coefficient fitting curve function expression	Cl_0	lift coefficient of the wing when the aileron maintains the original aileron deflection angle and the synthetic jet exciter is not working
T_2	end time selected when calculating effective value after the lift coefficient curve changes periodically	h	height
T_1	start time selected when calculating the effective value after the lift coefficient curve changes periodically	SJA	Synthetic Jet Actuator
Cl_b	chord When the aileron is deflected by a certain angle and the synthetic jet exciter is turned on, the lift coefficient of the wing	na	no actuator
		a	actuator

1. INTRODUCTION

Recently, active flow control (AFC) has gradually become the main research direction in the field of hydrodynamics. AFC is the main method to change the flow field properties through controlled equipment (Wang *et al*. 2020). Airflow separation on the wing surface is a typical adverse phenomenon in aircraft flight. The state of the boundary layer near the aircraft control surface will directly affect the torque of the aircraft, which will seriously affect the efficiency of the control surface. Therefore, the flow separation near the boundary layer is one of the most common problems in the field of flow field control near the wing (Hasegawa and Obayashi 2018).

Synthetic jet actuator (SJA) has attracted extensive attention because it has the advantages of small volume, lightweight, no additional injection source, simple manufacturing technology, and the ability to generate momentum without the fluid pipeline. Therefore, SJA is the main development direction in the field of active flow control. It is generally considered to be the most potent active flow control method (Feng *et al*. 2019). By using SJA, the lift coefficient of the wing can be effectively improved, that is, the lift generated by the wing can be significantly increased.

In this paper, the effect of SJA on the control efficiency of the wing is studied. Importantly, the moment in the rolling direction is determined by the lift generated by the aileron. When the wing lift coefficient is significantly increased, the control efficiency of the aileron is also improved. In other words, when the aileron deflects at the same angle, the lift of the wing using the SJA is much greater than that of the wing without the SJA.

The research of Zhang and Torres showed that the SJA had a strong ability to control the high-speed flow field (Zhang *et al*. 2018; Torres 2017). The experiments of Neuberger and Wygnanski, Bar Sever and Seifert could confirm the following conclusions: the separation of airflow could be delayed or even prevented completely by the method of synthetic jet (Neuburger and Wygnanski 1988; Bar-Sever 1989; Margalit *et al*. 2005). Recent evidence showed that the maximum outlet velocity of SJA was the most important factor affecting the control effect of gas flow separation (Zheng *et al*. 2005).

In Zhang's research, it was proposed to numerically simulate the flow separation control of the NACA-0018 airfoil at 10° angle of attack and Reynolds number Re =10000 (Zhang and Samtaney 2015). The influence of excitation frequency on flow separation control was quantified. For all flow separation control cases, the aerodynamic performance of the airfoil was analyzed based on the proportion of lift and vortex shedding. For all flow control cases, the aerodynamic performance of the airfoil was improved, and F=1.0 (the case with low excitation frequency) was the best case. Wang used a synthetic jet incompressible flow with a low Reynolds number to control the pitching direction of the NACA-0012 airfoil and improved its aerodynamic performance. The results showed that based on the results of numerical simulation, adjusting the phase angle to change the suction time of synthetic jet could obtain the best effect of increasing lift and reducing resistance (Wang and Wu 2020). Holman's paper introduced the research on controlling the airflow separation phenomenon in the boundary layer under the condition of Reynolds number Re=100000. When the angle of attack of the wing was 12°, the joint action of two SJA is used. The results showed that the control effect of airflow separation did not seem to be significantly affected by the opposite phase (Holman *et al*. 2003). Goodfellow experimentally investigated the control effect of a SJA on the shear layer flow separation at the tail of NACA-0025 airfoil at an angle of attack of 5° and Reynolds number Re=100000. The results indicated that the momentum coefficient was the main parameter affecting the effect of AFC (Goodfellow *et al*. 2013). Applying a specific SJA higher than the momentum coefficient, it would produce 50% resistance. Cattafesta adopted an active control method to suppress the cavity resonance noise caused by low Reynolds number (MA<0.2) flow, and found that the synthetic jet could effectively reduce the noise (Cattafesta *et al*. 1997, Cattafesta *et al*. 1999).

Flow control with efficient high-speed can achieve safe and maneuverable high-speed flight (Wang *et al*. 2012). When the effect of synthetic jet on lift coefficient was investigated, it was found that the results obtained by different test methods were completely different. Under some conditions, such as a certain angle of attack and a certain Reynolds number, little research had been done on the effect of synthetic jet on aileron efficiency under a certain working condition.

According to the above, previous researchers had studied the influence of synthetic jets on determining parameters and airfoil. However, the application of synthetic jet actuators in flight control was rarely investigated by researchers, and the effect of synthetic jets on the efficiency of aircraft control surface was hardly analyzed. The numerical simulation in this paper uses synthetic jet control measures to improve the flow field near the aileron at the trailing edge of the wing, and reveal the influence of different conditions on the control efficiency of the active flow control measures, to effectively enhance the maneuverability of the aircraft in the roll direction. At the same time, the control efficiency of the corresponding aileron has also been significantly improved.

To investigate the synergistic effect of SJA on wing control surface efficiency, due to the particularity of the wing problem, the aileron efficiency of aircraft can be reflected in the variation of wing rolling torque, and the wing model can be simplified into a two-dimensional profile model. The magnitude of the rolling moment also becomes the magnitude of the lift of the corresponding profile. According to the lack of previous research, it is decided that in this paper, the variation of the lift coefficient generated by the wing when the aileron deflects a certain angle (3°~9°) and the synthetic jet is used will be

compared. The influence of different synthetic jet actuators on the efficiency of the aileron is further studied.

2. PHYSICAL MODEL AND ACCURACY VERIFICATION

2.1 Physical Model

1) Wing and flow field

The EPPLER555 wing model is selected for this numerical simulation. The chord length of the EPPLER555 wing is set as L, the maximum thickness of the wing is 0.16 L, the SJA is installed on the upper surface of the wing aileron, and the outlet width of the SJA is 0.01L. The jet direction generated by the SJA is tangential to the upper surface of the aileron and points to the trailing edge of the wing. When the control surface of the wing deflects, the outlet direction of the SJA deflects as well. Therefore, the included angle between the outlet velocity direction of the SJA and the upper surface of the wing is always 0°.

The research model is a wing part of the fixed wing aircraft, the wing control surface is the aileron, and the physical model of the wing and flow field is shown in Fig. 1. The whole rectangular area is the flow calculation domain, the left is the velocity inlet, the mainstream velocity is 200 m/s, and the air flow is from the left. The upper and lower sides are also velocity inlets, with a horizontal velocity of 200 m/s and a vertical velocity of 0 m/s, that is, the velocity direction is consistent with the direction and size of velocity inlets. The right side is the pressure outlet, and the EPPLER555 wing model is in the middle of the flow field. A SJA with a width of 0.01L is added to the front of the upper surface of the EPPLER555 aileron.

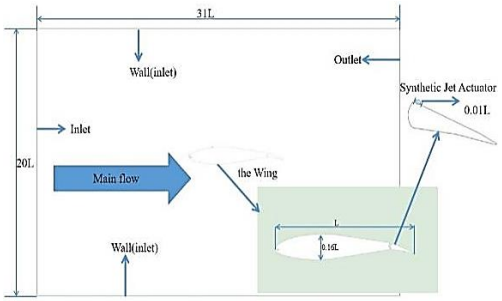

Fig. 1. EPPLER555 wing model.

2) Boundary conditions

Boundary conditions of synthetic jet actuator: The outlet velocity of the SJA is a sinusoidal function varying with time, as expressed in Eq.1.

$$V_{SJA} = V_{Max} \times sin(\omega t + \varphi) \quad (1)$$

In Eq.1, V_{Max} represents the maximum outlet velocity of the synthetic jet actuator, ω determines the excitation frequency of the synthetic jet actuator, and the excitation frequency f = ω/2π. Meanwhile, the phase φ determines whether the synthetic jet actuator is in the "suction" stage or "blowing" stage when it starts working and during the flow.

When the aileron deflection angle is greater than 3°, the lift coefficient can be significantly improved using the SJA. A larger aileron deflection angle increases the angle of attack, and the influence of the SJA on lift coefficient gradually decreases with the increase in the angle of attack. Therefore, the aileron deflection angle of 3˚-9˚ is selected. The two important parameters of the SJA are the maximum outlet velocity V_{Max} and excitation frequency f.

The velocity inlet of the flow field is set to 200 m/s, and the Reynolds number is 1.37×10^7. To study the influence of the synthetic jet actuator maximum outlet velocity on the lift coefficient, the excitation frequency of the actuator is fixed at 200/π Hz, and the maximum velocity at the outlet of the synthetic jet actuator is set to 200 m/s, 100 m/s, 50 m/s, 25 m/s, 15 m/s, and 300 m/s in turn. When studying the influence of excitation frequency f, the maximum outlet velocity of the synthetic jet actuator is set to 200 m/s. The excitation frequencies of 200/π Hz, 100/π Hz, 50/π Hz, 25/π Hz and 12.5/π Hz are used. Table 1 lists the parameter settings table of the SJA.

Table 1 Parameter of synthetic jet actuator

Deflection angle of aileron	The exit velocity of the SJA（V_{Max}）	Excitation frequency of SJA（f）
3˚, 4˚, 5˚, 6˚, 7˚, 8˚, 9˚	15m/s, 25m/s, 50m/s, 100m/s, 200m/s, 300m/s	12.5/πHz, 25/πHz, 50/πHz, 100/πHz, 200/πHz

3) Mesh

Like the verification calculation method, the unstructured grid generation is faster and more automated. To obtain better data near the wing and aileron, the grid in this area is encrypted. A 20-layer grid is divided around the wing as the boundary layer, the front of the aileron upper surface is the position of the SJA, and the grid at the synthetic jet actuator is densified.

As shown in Fig. 2, it is the grid when the aileron deflection angle is 3°:

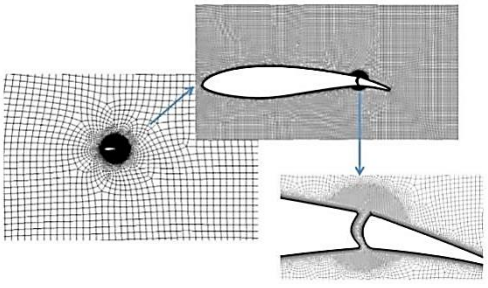

Fig. 2. Wing profile grid and show details.

The grid drawing method of the aileron deflection angles of 4°-9° is the same as that when the aileron deflection angle is 3° and not repeated.

2.2 Turbulence Model

The SST k-ω model has a wide range of applications., as the hybrid model is widely used in engineering. The SST k- ω model is a combination of the k-ω model and k-ε model, where the k-ε model can better simulate the fully developed turbulence far from the wall. When solving the boundary layer problem under various pressure gradients, the k-ω model is more accurate. In addition to the advantages of stability and high accuracy, the SST k-ω model can also address the transmission of turbulent shear stress in the reverse pressure gradient and separation boundary layer. Because of these advantages the SST k-ω model can better predict more complex flow conditions, such as reverse pressure gradient and separated boundary layer. Therefore, in this paper, the SST k-ω model is chosen to reduce the influence of shear stress and complex flow conditions.

Equation 2 is the continuity equation, which is a form of mass conservation expression. The continuity equation is applicable whether the fluid is compressible or incompressible. The source phase S_m is the mass added to the continuous phase by a dilute phase (e.g., a liquid evaporates into gas) or a mass source phase. (user-defined)

$$\frac{\partial p}{\partial t}+\frac{\partial}{\partial x}(\rho u_i)=S_m \tag{2}$$

Equation 3 is the N-S equation. In the inertial coordinate system, the momentum conservation equation in the i direction is:

$$\frac{\partial}{\partial t}(\rho u_i)+\frac{\partial}{\partial x_j}\left(\rho u_i u_j\right)=-\frac{\partial P}{\partial x_i}+\frac{\partial \tau_{ij}}{\partial c_j}+\rho g_i+F_i \tag{3}$$

where P is the static pressure, $\tau_{ij}$is the stress tensor, $\rho g_i$is the volume force of gravity, and F_i is other volume forces.

2.3 Accuracy Verification

To verify the accuracy of the physical and turbulence models in this study, we select the experimental results of NACA0012 airfoil lift coefficient varying with angle of attack obtained by the Institute of Fluid Science of Tohoku University in Japan (Hasegawa H and Obayashi 2018). The drawing method of the NACA0012 wing simulation grid is the same as that of EPPLER555, which is described above. The flow field area is a rectangle with a length of 31 L and a width of 20 L. The NACA0012 wing model is located at the center of the rectangle. Meanwhile, the chord length of the NACA0012 wing model is L = 1 m, and the chord length is the characteristic length of the wing.

Figure 3 illustrates a comparison between the lift coefficient curve obtained by the Fluid Science Research Institute of Tohoku University of Japan and the experimental value of this numerical simulation at different angles of attack. It can be seen from the figure that under different angles of attack, the lift coefficient value obtained in this paper is mostly consistent with that of NACA0012 obtained by the Institute of Fluid Science of Tohoku University. The maximum deviation of the lift coefficient is only 3.46%, indicating that the calculation in this paper meets the accuracy requirements. The physical model and numerical methods can be used for subsequent calculations.

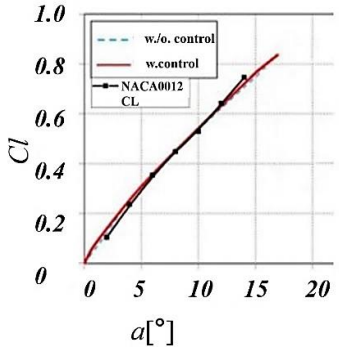

Fig. 3. Comparison of NACA0012 wing lift coefficient (Re=1.5*106).

3. Results and Discussion

Under the effect of the SJA with different maximum outlet velocities, it can be concluded through the numerical simulation of the EPPLER555 wing model (using Fluent) that when the outlet velocities of the SJA differ, the variation values of the wing lift coefficient with time are also different.

When the aileron deflects at the same angle, actuators with different excitation frequencies are used on the wing. Under the effect of the SJA with different excitation frequencies, the change in lift coefficient of the wing with time under corresponding working conditions is obtained.

The addition of the SJA can improve the aileron control efficiency of the EPPLER555 wing. Thus, suggestions can be obtained for the EPPLER555 wing using the SJA by comparing the improvement in the aileron control efficiency when using SJA with different parameters.

When synthetic jet actuators with different parameters are used, the cftool in MATLAB is used to fit the lift curve of the wing. After analysis, the wing lift coefficient curve is close to the second-order Fourier function curve. Because the exit velocity of the synthetic jet actuator changes periodically, the lift coefficient of the wing also changes periodically after the SJA is employed. When the corresponding SJA works, the effective value of the wing lift coefficient can be calculated according to Eq.4, and the second-order Fourier function is used to replace the wing lift coefficient.

$$Cl_{eff}=\frac{\int_{T_1}^{T_2}L(t)dt}{T_2-T_1} \tag{4}$$

To describe the use of SJA on the wing more conveniently, the following naming method is specified. When the aileron deflection angle is 4° and the SJA is not used on the aileron, this situation is named 4na (no actuator). When the SJA with maximum outlet velocity is 200 m/s and the

excitation frequency f = 200/π Hz is used on the aileron with an aileron deflection angle of 4°, the working condition is named 4a-200-400 (f = 400/2π). At each aileron deflection angle, the naming method of the SJA with other parameters is the same.

By calculating the effective lift coefficient generated by the aircraft wing, the improvement range of the control surface efficiency of the aircraft aileron can be reflected. By analyzing the pressure and vorticity changes of the flow field near the aileron, the author's assumption of the change in the lift coefficient and the reason for the improvement of control efficiency can be verified.

3.1 Comparison of Effective Values of Lift Coefficient with SJA and Without SJA (3°~9° Aileron Deflection Angle)

1) Effective value of lift coefficient for changing the maximum outlet velocity of SJA

As shown in Table 2, when the SJA with different maximum outlet velocities is used, the effective value of the lift coefficient is generated by the wing when the aileron deflects at different angles.

Table 2 also shows that under different aileron deflection angles, the employment of the SJA increases the lift coefficient of the wing. When the aileron deflection angle is 3° to 7°, the use of the SJA with a maximum outlet velocity of 15 m/s effectively improves the lift coefficient. For example, when the aileron deflection angle changes from 3° to 4°, and the SJA is not used, the lift coefficient only increases by 0.0092. When the SJA with the maximum outlet velocity of 15 m/s is used, the lift coefficient at the aileron deflection angle of 4° is 0.6592, which increases by 0.161 compared with that of 3°. For cases in which the aileron deflection angle is greater than 7°, the smaller outlet velocity does not meet the requirements for improving the lift coefficient. It is necessary to use a SJA with a maximum outlet velocity greater than 50 m/s. After using such SJA, the lift coefficient increases by 0.1326 when the aileron deflection angle changes from 7° to 8°. When the SJA is not used, and the aileron deflection angle changes from 7° to 8°, the lift coefficient increases by only 0.0049. For other aileron deflection angles, the lift coefficient of the wing is considerably improved by using an appropriate SJA.

Figures 4 (a)-(f) show the wing lift curves with SJA, without SJA, and with SJA reaching different maximum outlet velocities when the aileron deflection angle is deflected by 1°.

As shown in the figures above, after using the SJA, the lift coefficient curve generated by the wing under different aileron deflection angles changes periodically with time. In a working cycle of the SJA, the lift coefficient first increases to a maximum value, decreases slightly, increases again to the maximum value in a cycle, and finally, decreases to the minimum value to end a complete cycle. The larger the outlet velocity, the greater the fluctuation range of the lift coefficient curve is. When the maximum outlet velocity of the SJA is greater than that of the incoming flow (that is, when the SJA with the maximum outlet velocity of 300 m/s is used), the lift coefficient curve is lower than the wing lift coefficient curve when the SJA is not used at some time. These phenomena show that when the SJA with the maximum outlet velocity slower than the incoming velocity is used, the lift coefficient and control surface efficiency of the wing aileron can be improved more effectively.

2) Effective value of lift coefficient for changing the excitation frequency of SJA

For SJAs with different excitation frequencies, the effective values of the lift coefficient generated are presented in Table 3 when the aileron deflects the corresponding angles.

Table 2 Effective values of the lift coefficient by changing the maximum outlet velocity

RDA / V_{Max}	3°	4°	5°	6°	7°	8°	9°
Without SJA	0.4919	0.5011	0.4893	0.5223	0.5363	0.5412	0.5551
15m/s	-	0.6529	0.6992	0.7012	0.7145	-	-
25m/s	-	0.6482	0.6918	0.6943	0.7093	-	-
50m/s	-	0.6369	0.6661	0.6807	0.6961	0.6689	0.5637
100m/s	-	0.6107	0.6251	0.6559	0.6708	0.6622	0.634
200m/s	-	0.5931	0.6219	0.6456	0.6718	0.6781	0.6864
300m/s	-	0.5917	0.6201	0.646	0.6728	0.6841	0.7001

Table 3 effective values of the lift coefficient by changing the excitation frequency

RDA / f	3°	4°°	5°	6°	7°	8°	9°
Without SJA	0.4919	0.5011	0.4893	0.5223	0.5363	0.5412	0.5551
12.5/πHz	-	0.5863	0.6048	0.6235	0.6556	0.6212	0.6652
25/πHz	-	0.6208	0.6278	0.675	0.6791	0.6013	0.7145
50/πHz	-	0.6029	0.6247	0.6514	0.6756	0.5888	0.6841
100/πHz	-	0.6054	0.6199	0.6511	0.6705	0.5876	0.6809
200/πHz	-	0.6107	0.6251	0.6559	0.6708	0.6622	0.634

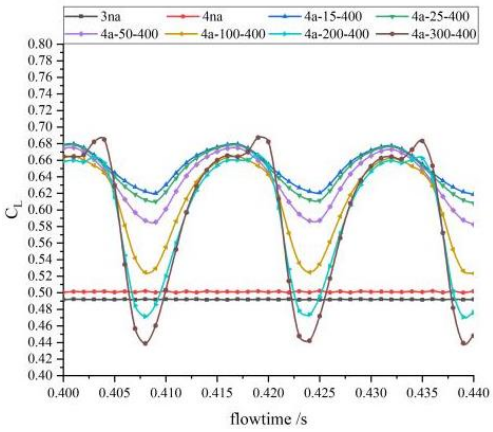

Fig. 4. (a) Lift coefficient of 3˚~4˚

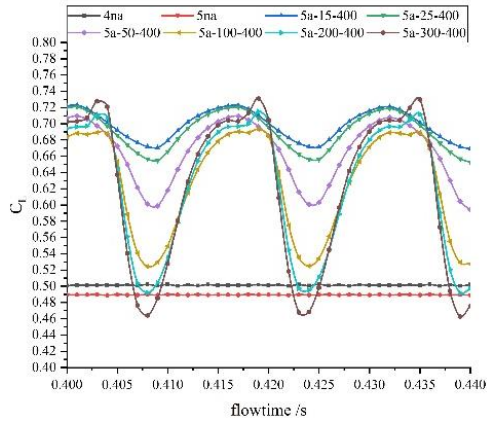

Fig. 4. (b) Lift coefficient of 4˚~5˚

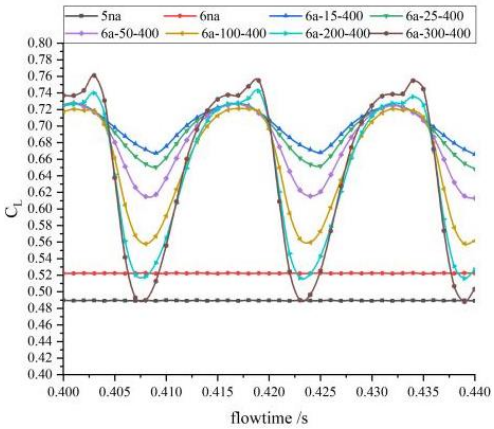

Fig. 4. (c) Lift coefficient of 5˚~6˚

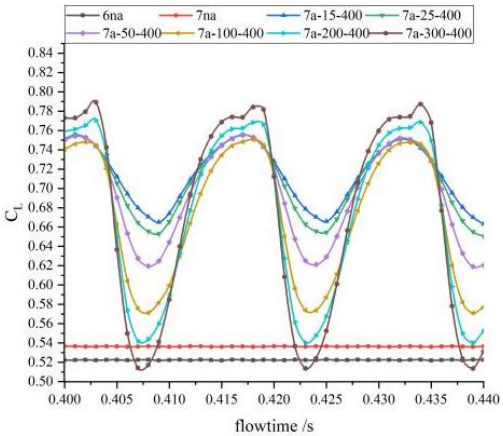

Fig. 4. (d) Lift coefficient of 6˚~7˚

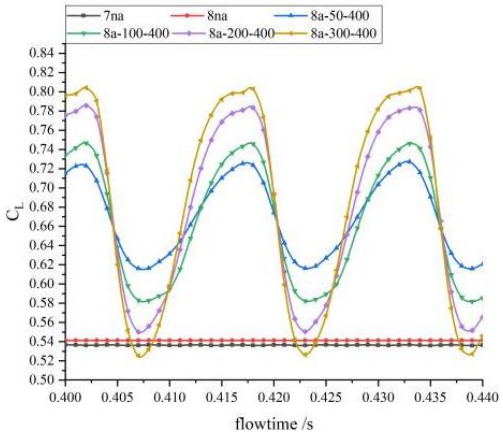

Fig. 4. (e) Lift coefficient of 7˚~8˚

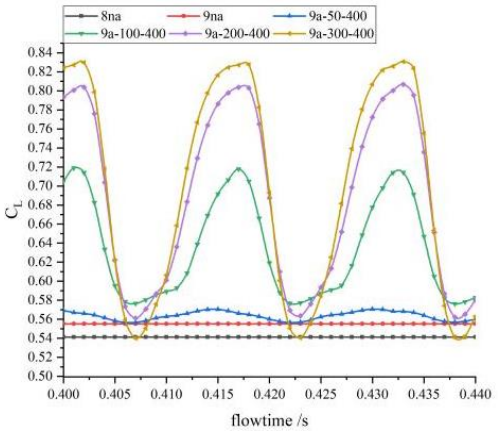

Fig. 4. (f) Lift coefficient of 8˚~9˚

Table 3 shows that when the aileron deflection angle is 3° to 9°, the use of the SJA effectively increases the lift coefficient, and the lift coefficient generated by the wing increases with a growth in the excitation frequency of the SJA. In this simulation, the excitation frequency with the best effect is 200/π Hz. For example, when the aileron deflection angle changes from 3° to 4°and the SJA is not used, the lift coefficient increases from 0.4919 to 0.5011. After using the SJA with an excitation frequency of 200/π Hz, the lift coefficient generated by the wing at 4° increases to 0.6107. Subsequently, the change in the lift coefficient generated by the wing increases from 0.0092 to 0.1188. The variation behavior of the lift coefficient is the same in the case of other aileron deflections. When the aileron deflection angle is larger than 7°, the SJA with a small excitation frequency cannot stably improve the aileron efficiency. For example, except for the aileron deflection of 9° and synthetic jet actuator with an excitation frequency of 25/π Hz, the lift coefficient of the wing is relatively small.

As shown in Figs. 5 (a)-(f), when the aileron deflection angle deflects by 1°, for example, when

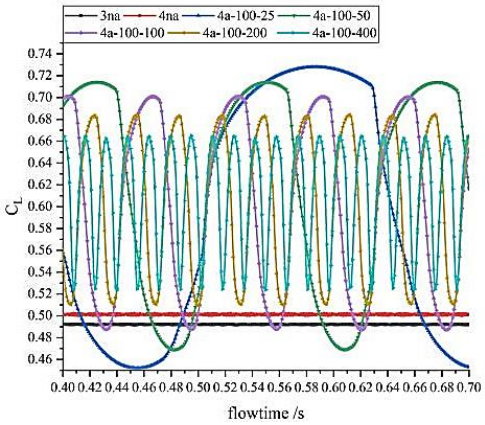

Fig. 5. (a) Lift coefficient of 3˚~4˚.

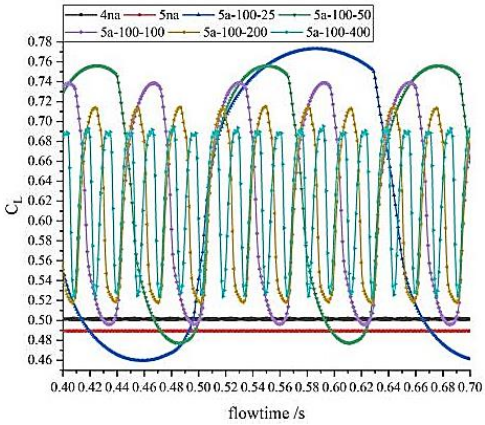

Fig. 5. (b) Lift coefficient of 4˚~5˚.

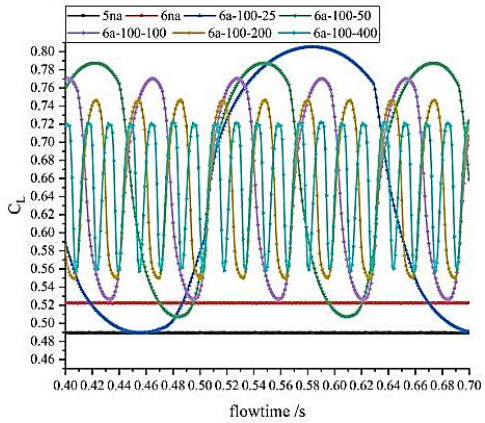

Fig. 5. (c) Lift coefficient of 5˚~6˚.

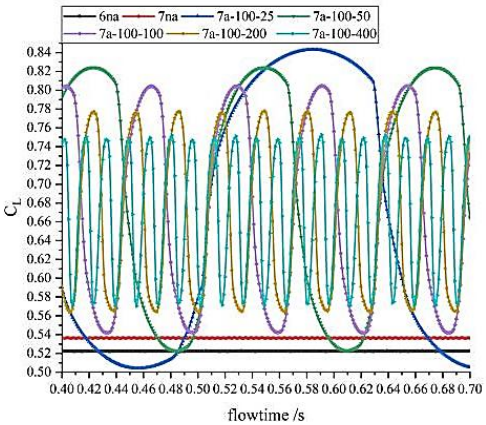

Fig. 5. (d) Lift coefficient of 6˚~7˚.

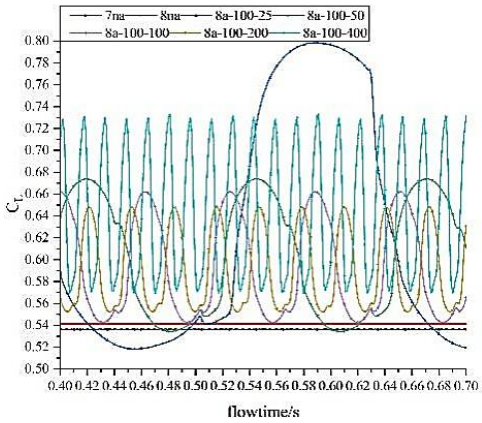

Fig. 5. (e) Lift coefficient of 7˚~8˚.

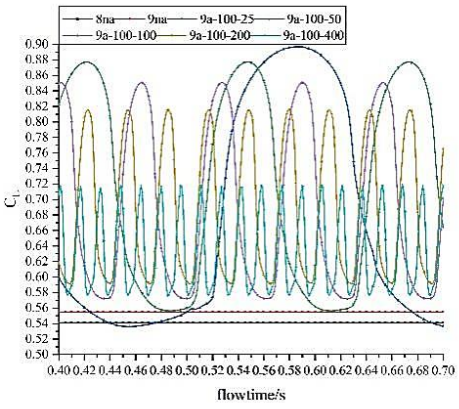

Fig. 5. (f) Lift coefficient of 8˚~9˚.

the aileron deflection angle changes from 3° to 4°, Fig. 5 (a) shows the lift curve generated by the wing without the synthetic jet actuator and the lift coefficient generated by the wing with the synthetic jet actuator with different excitation frequencies.

As shown in the figures above, after using the SJA, the lift coefficient curve generated by the wing under different aileron deflection angles changes periodically with time. When the excitation frequency is greater than 100/π Hz, curve characteristics of the lift coefficient generated by the wing in a complete cycle first increases to the maximum value, decreases slightly, increases again to the maximum value in the cycle, and finally decreases to the minimum value. When the excitation frequency of the SJA is less than 100/π Hz, the lift coefficient first increases rapidly, and then decreases in a working cycle. When the lift coefficient reaches the maximum value, it decreases slowly and then drops to the minimum value at a certain point, ending the cycle. When the excitation frequency of the SJA is higher, the change period of the lift coefficient curve is smaller, and changing the excitation frequency has little influence on the fluctuation amplitude of the lift coefficient curve.

However, to better stabilize the change in the lift coefficient curve, the SJA with a higher excitation frequency should be used in a smaller period.

3.2 Comparison of Aileron Surface Efficiency

The efficiency of the aileron is defined as the torque generated by the corresponding control surface when the aileron deflects by a certain angle. For example, when the torque generated by the aileron deflecting by the same angle is greater, the aileron is likely of higher efficiency. When studying the efficiency of the control surface on the wing, the moment is the rolling moment, and the force determining the rolling moment is the lift generated by the wing. Because the model is two-dimensional, the rolling moment on a section of the wing can be reflected by the lift on that section. Therefore, the control surface efficiency of the aileron is measured by the lift coefficient of the wing. Here, the authors propose Eq.5 to calculate the additional aileron efficiency.

$$\Delta\eta = \frac{(Cl_b - Cl_0) - (Cl_a - Cl_0)}{Cl_a - Cl_0} \tag{5}$$

According to Eq. 5 and the effective lift coefficient values in Tables 2 and 3, we calculate the improvement degree of aileron the efficiency using synthetic jet actuators with different parameters when the aileron deflects by the same angle. By quantifying the improvement in aileron efficiency when the aileron deflects by every 1° and comparing the effects of various parameters on aileron efficiency, the SJA parameters. For maximizing aileron efficiency can be obtained.

1) Aileron efficiency at different maximum exit speeds

Table 4 presents the average increase in aileron control surface efficiency when using SJAs with different maximum outlet velocities

The data presented in Table 4 are according to the calculation formula of the average increase in the aileron efficiency proposed above. The data, show that the aileron efficiency of the wing can be improved using the SJA. For example, when the aileron deflection angle changes from 3° to 4°, the aileron efficiency is increased by 30.86% when the maximum outlet velocity of 15 m/s. When the SJA with the maximum outlet velocity of 300 m/s is used, the aileron efficiency is also improved by 18.418%. When the aileron deflection angle is 3° to 7°, the behavior of using the SJA with different maximum outlet velocities is the same, that is, using a 15 m/s SJA will improve the aileron efficiency. When the aileron deflection angle is greater than 7°, the aileron deflection angle changes from 7° to 8° and from 8° to 9°, and the SJA used requires a large maximum outlet velocity (more than 25 m/s) to effectively improve the aileron efficiency. In the simulation, the SJA with a minimum of 50 m/s is selected. According to the calculation, the greater the maximum outlet velocity of the SJA used, the greater the improvement of the aileron efficiency. For example, when the aileron deflection angle changes from 8° to 9°, the aileron efficiency increases by 1.589% using the SJA with the maximum outlet velocity of 50 m/s. Moreover, when using the SJA with the maximum outlet velocity of 300 m/s, the control surface efficiency of the wing improves by 26.646%. However, the values are still not as good as those obtained using the SJA with the maximum outlet velocity of 15 m/s at a small aileron deflection angle (3°-7°), where the aileron efficiency improves by at least 30%.

2) Aileron efficiency at different excitation frequencies

Table 5 presents the average increase in the aileron control surface efficiency when using SJAs with different excitation frequencies.

Table 4. Improved value of aileron efficiency by changing maximum exit velocity

RDA Change / V_{Max}	3˚～4˚	4˚～5˚	5˚～6˚	6˚～7˚	7˚～8˚	8˚～9˚
15m/s	30.86%	43.13%	36.56%	34.12%		
25m/s	29.90%	41.65%	35.15%	33.12%		
50m/s	27.61%	36.52%	32.37%	30.60%	23.81%	1.59%
100m/s	24.15%	28.34%	27.30%	25.75%	22.56%	14.57%
200m/s	18.70%	27.67%	25.20%	25.94%	25.53%	24.26%
300m/s	18.42%	27.34%	25.28%	26.13%	26.65%	26.79%

Table 5. Improved value of aileron efficiency by changing excitation frequency

RDA Change / f	3˚～4˚	4˚～5˚	5˚～6˚	6˚～7˚	7˚～8˚	8˚～9˚
12.5/πHz	17.321%	24.287%	20.683%	22.841%	14.917%	20.344%
25/πHz	24.334%	28.876%	31.208%	27.341%	11.206%	29.453%
50/πHz	20.695%	28.258%	26.385%	26.670%	8.876%	23.536%
100/πHz	21.203%	27.230%	26.323%	25.694%	8.652%	23.245%
200/πHz	24.151%	28.338%	27.304%	25.751%	22.562%	14.579%

The data in Table 5 are obtained according to Eq.5. According to the data, the aileron efficiency greatly improves when the aileron deflection angles range from 3° to 7°, and the SJA with a high excitation frequency is used on the wing. For example, when the aileron deflection angle is changed from 3° to 4°, and the SJA with the excitation frequency of 12.5/π Hz is used, the aileron efficiency increases by 17.321%. When using the SJA with 200/π Hz, the efficiency of the aileron increases by 24.151%. In this simulation, when each aileron angle is deflected, the SJA with an excitation frequency of 25/π Hz improves the aileron efficiency to the greatest extent. The SJA with this frequency improves the aileron efficiency by at least 20%. When the SJA with an excitation frequency greater than 25/π Hz is used, such as (50/π Hz, 100/π Hz), the increase in aileron efficiency will be reduced. When the aileron deflects by 8°, only the SJA with an excitation frequency of 200/π Hz achieves good results, unlike the SJA with other excitation frequencies results. When the aileron deflects by 9 °, the SJA with the excitation frequency of 25/π Hz still works adequately. When using the SJA with other excitation frequencies, the effect is similar to that under the deflection angle of other ailerons.

3.3 Analysis of Aerodynamic Characteristics and Flow Field

In the wing flow field, a closed circulation is formed to surround the wing. The amount of circulation around the wing τ is 0 when the wing is stationary. When the fluid blows over the airfoil surface, the circulation τ is close to the wing. In this case, no boundary layer can be formed on the surface (viscosity takes some time to take effect), and the circulation around the wing is still 0. At this time, the stagnation point is on the upper wing rather than at the trailing edge. After a period, the air flow on the lower wing bypasses the trailing edge and flows to the upper wing. Owing to the high velocity and low pressure at the trailing edge, a large inverse pressure gradient occurs on the wing between the trailing edge and the stagnation point, resulting in boundary layer separation. These boundary layers leave the airfoil and produce counterclockwise vortices +τ, which are called the starting vortices and move downstream with the fluid. During the motion of the starting vortex, the contour of the closed circulation gradually increases and always surrounds the wing and the starting vortex. According to Helmholtz's law of vortex conservation, the circulation around the wing is always 0. thus, a clockwise circulation should be generated on the wing -τ. Owing to the action of -τ, the airflow velocity on the upper wing increases and the stagnation point moves to the trailing edge. However, this above process continues if the stagnation point remains on the upper wing surface. The constant counter clockwise starting vortex is dragged downstream, the clockwise circulation around the wing continues to increase, and the stagnation point continues to move backward until it reaches the trailing edge of the wing. At this time, the upper and lower airfoils meet at the trailing edge, and the wing advances at a constant velocity, the starting vortex is left behind, and the circulation around the airfoil is constant.

The eddy representing the area around the wing is called an attached eddy because it is always attached to the wing. In this simulation, the maximum deflection of the aileron is 9°, and the corresponding wing angle of attack is approximately 2.5°. At a small angle of attack, no attached vortex falls off.

The authors speculates that the reason may be that during the operation of the SJA, because the outlet velocity of the SJA is a sinusoidal function varying with time, the outlet direction of the SJA is tangential to the direction of the upper wing, and the outlet is close to the wing. The direction of the jet is opposite to the flow direction of the attached vortex near the wing. Therefore, when the outlet velocity of the SJA increases, the strength of the attached vortex decreases. On the contrary, when the outlet velocity of the SJA reduces, the strength of the attached vortex increases because the total circulation is constant.

Observing the outlet velocity of the SJA and comparing the change period of lift coefficient with the working period of the SJA, it is found that the effect of the SJA is delayed relative to the change in the outlet velocity of the SJA.

Figure 6 shows the lift coefficient curve of the wing when the deflection angle of the wing control surface is 4° and when the SJA has a maximum outlet velocity of 200 m/s and an excitation frequency of 200/π Hz.

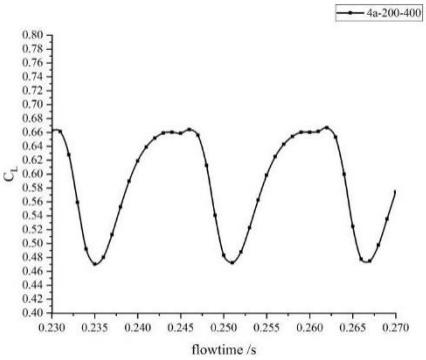

Fig. 6. Lift coefficient graph.

Figures 7 and 8 illustrate the changes in vorticity and pressure on the wing surface during the working cycle of the SJA when the aileron deflection angle is 4° and the SJA is with a maximum outlet velocity of 200 m/s and an excitation frequency of 200/π Hz. The working cycle from t = 0.236 s to t = 0.251 s is selected for analysis.

The beginning of a working cycle of the SJA is at 0.236 s, and 0.236 s to 0.251 s is a complete working cycle of the SJA. Then 0.236 s to 0.244 s is the "blowing" stage of operation. Figs. 7 (a)-(c) show the pressure field near the aileron during the "blowing". When the SJA is in the "blowing" process, the lift coefficient of the wing is mainly determined by the pressure difference between the upper wing surface and the lower wing surface. As can be seen from

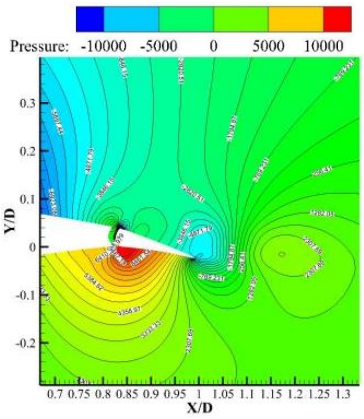

Fig. 7. (a)t=0.236s

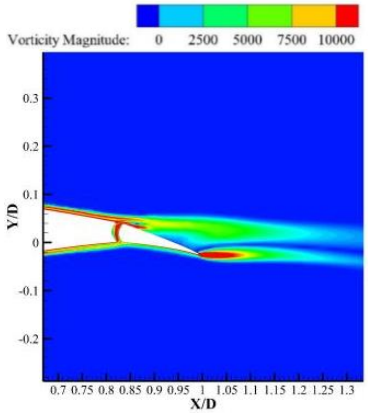

Fig. 7. (1) t=0.236s.

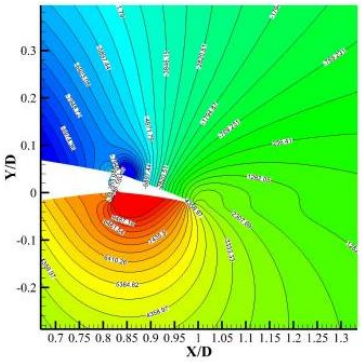

Fig. 7. (b)t=0.240s

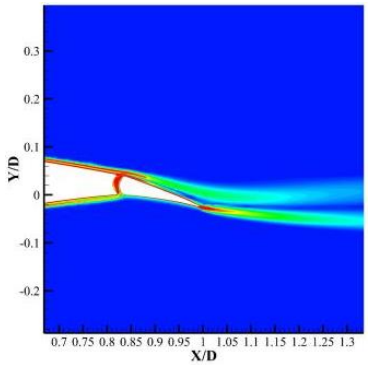

Fig. 7. (2)t=0.240s .

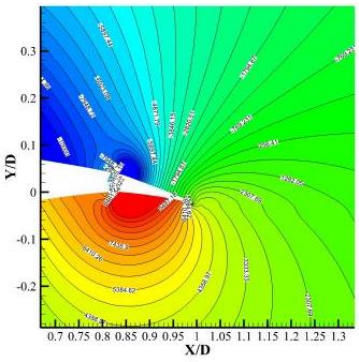

Fig. 7. (c)t=0.244s

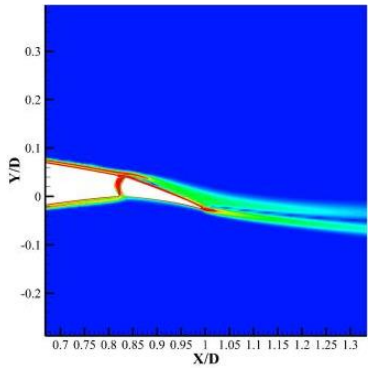

Fig. 7. (3)t=0.244s.

Fig. 7. "Blowing" stage.

Figs. 7 (a)-(c), between 0.236 s and 0.244 s, the pressure difference between the upper and lower surfaces of the wing gradually increases. Hence, the lift coefficient also increases with the argument of the pressure difference. Figs. 7 (1)-(3) show the change in vorticity intensity near the aileron during "blowing". In this half cycle, the vortex strength changes slightly and has no obvious effect on the lift coefficient.

As shown in Fig. 8, an attached vortex whose size changes with time exists when the SJA is in the "suction" process. From 0.245 s to 0.247 s, the intensity of the attached vortex increases gradually. Additionally, the attached vortex starts decreasing after 0.247 s until it reaches the minimum at 0.251 s. At this point, the complete working cycle has been passed for the SJA. When the SJA is in the 'blowing' stage again, the attached vortex counteracts the jet ejected by the SJA again, and the SJA enters a new working cycle.

When the SJA is in the "suction" process, the attached vortex on the wing surface appears again. According to the Kutta Joukowski theorem, the buoyancy of a rotating cylinder or an object in a flow field with different upper and lower velocities can be calculated. The buoyancy is equal to the product of the relative velocity between the cylinder and the fluid, the fluid density, and the circulation. When the airflow around the two-dimensional wing model is uniform and inviscid at a low velocity, the force perpendicular to the inflow direction on the length of

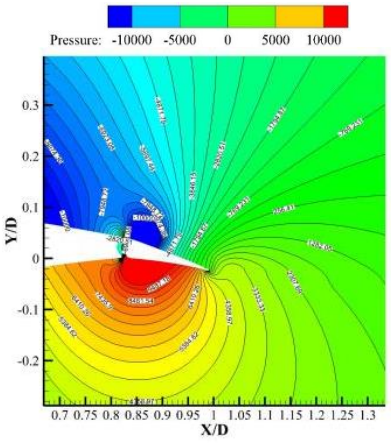

Fig. 8. (a)t=0.245s.

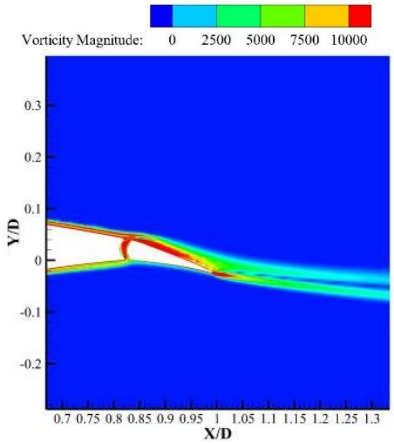

Fig. 8. (1)t=0.245s.

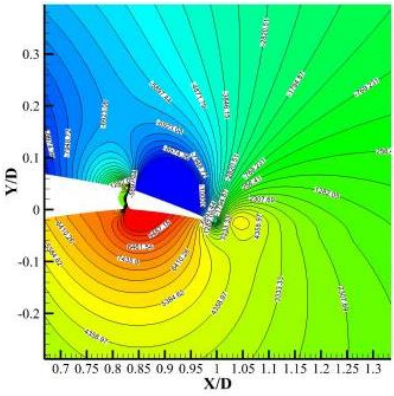

Fig. 8. (b)t=0.247s.

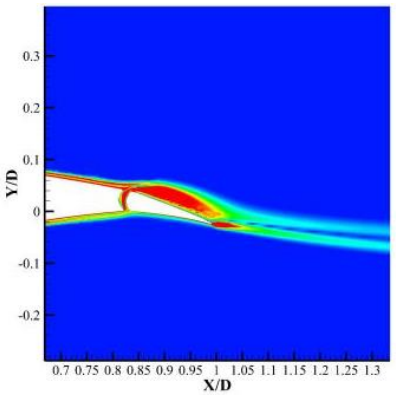

Fig. 8. (2)t=0.247s.

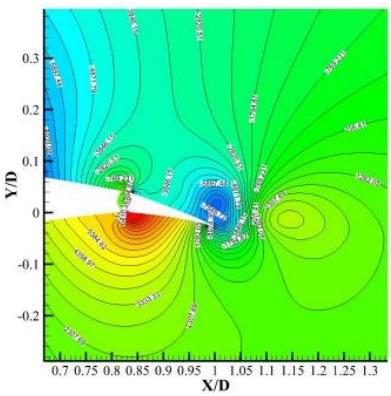

Fig. 8. (c)t=0.251s.

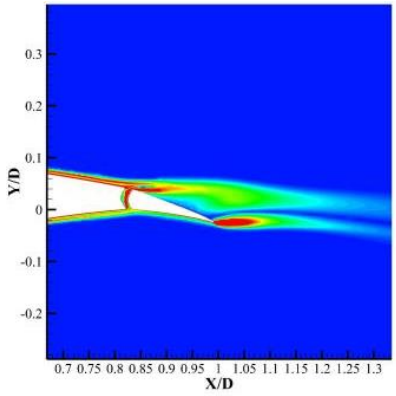

Fig. 8. (3)t=0.251s.

Fig. 8. "Inhalation" stage.

the two-dimensional wing element is equal to the product of the fluid density, inflow velocity, and circulation around the wing. This buoyancy is the lift. Stokes' theorem establishes that the circular linear motion along any closed curve L in space is equal to the integral of the curl on any curved surface formed by the curve. According to this theorem, the magnitude of circulation can be expressed by vortex strength. Therefore, when the relative velocity of the wing, air flow, and surrounding air density is the same, the lift generated by the wing is determined by the vortex strength.

Figures 8 (a) (b) (c) shows the pressure change near the aileron during "suction". The pressure difference between the upper and lower wings increases gradually from 0.245 s to 0.247 s and decreases gradually from 0.247 s to 0.251 s. Figs. 8 (1) (2) (3) shows the change in vorticity intensity near the aileron during "suction". At this stage, the lift coefficient of the wing is determined by the pressure difference between the upper and lower airfoils and the circulation (vortex strength), and the influence of the circulation on the lift is approximately 60%-70%. In the range of 0.245 s to 0.247 s, the vortex strength increases gradually as the lift coefficient increases. In the range of 0.247 s to 0.251 s, the vortex strength gradually decreases, and the lift coefficient also decreases.

According to the lift coefficient curve shown in Fig. 6, the above conclusion is verified at any time. As shown in Fig. 9, when 0.263 s is selected, the time is in the "suction" stage in the working cycle of the SJA, the vortex strength and lift coefficient reach the maximum, which is the same as the behavior described above.

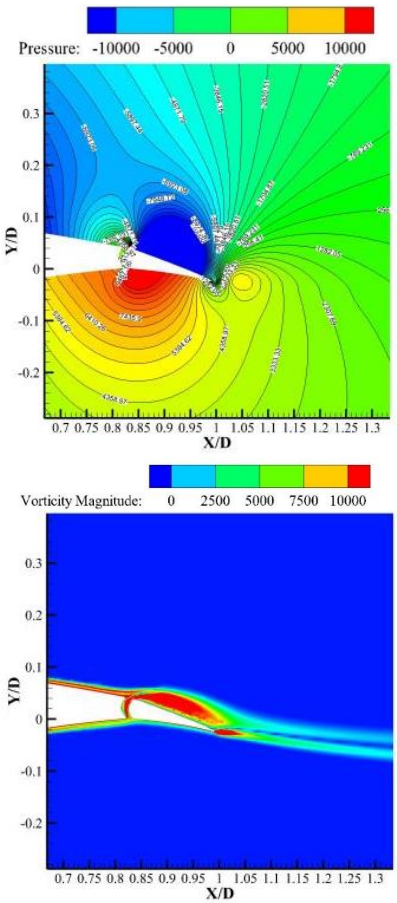

Fig. 9. Pressure and vorticity magnitude at t=0.236s.

4. CONCLUSION

This work, examined the changes in the lift coefficient and aileron efficiency of the EPPLER555 airfoil with the same aileron deflection angle after using various synthetic jet actuators.

1) Effect of maximum exit velocity of the SJA on aileron efficiency. Changing the maximum exit velocity of the SJA considerably affects the aileron efficiency. When the deflection angle of the control surface is 4°-7°, the aileron efficiency can be improved using a SJA with a maximum outlet velocity of 15 m/s to 300 m/s. When the deflection angle of the aileron is greater than 7°, the outlet velocity of the SJA used is greater than 50 m/s.

2) Maximum outlet velocity of the SJA increases from 15 m/s to 200 m/s, and the aileron control surface efficiency decreases with an increase in the maximum outlet velocity. When the maximum outlet velocity of the SJA is equal to or greater than the incoming velocity, the effect of improving the aileron efficiency is not obvious.

3) When the excitation frequency of the SJA increases, the aileron efficiency increases slightly. The larger the deflection angle of the aileron, the smaller the excitation frequency of the SJA required to improve the aileron efficiency to the same extent.

4) When the aileron deflection angle is 3° to 7°, a SJA with a maximum outlet velocity of 15 m/s and an excitation frequency of 25/π Hz is employed. The aileron efficiency can be increased by at least 27.939% for every 1° of aileron deflection. When the aileron deflection angle is greater than 7°, the aileron efficiency can be significantly improved by using a SJA with a maximum outlet velocity of 200 m/s and an excitation frequency of 200/π Hz. When the aileron deflection angle 7˚ to 8˚ the aileron efficiency can be increased by 25.527%.

REFERENCES

Bar-Sever, A. (1989). Separation control on an airfoil by periodic forcing. *AIAA Journal* 27(6), 820-821.

Cattafesta, L., D. Shukla, S. Garg and J. Ross (1999). Development of an adaptive weapons-bay suppression system. *5th AIAA/CEAS Aeroacoustics Conference and Exhibit* 1901.

Cattafesta, L., S. Garg, M. Choudhari and F. Li (1997). Active control of flow-induced cavity resonance. *28th Fluid Dynamics Conference* 1804.

Feng, J., Y. Lin, G. Zhu and X. Luo (2019). Effect of synthetic jet parameters on flow control of an aerofoil at high Reynolds number. *Sādhanā* 44(8), 1-10.

Goodfellow, S. D., S. Yarusevych and P. E. Sullivan (2013). Momentum Coefficient as a Parameter for Aerodynamic Flow Control with Synthetic Jets. *AIAA Journal* 51(3), 623-631.

Hasegawa, H. and S. Obayashi (2018). Active Stall Control System on NACA0012 by Using Synthetic Jet Actuator. *Journal of Flow Control, Measurement & Visualization* 7(1), 61-72.

Holman, R., Q. Gallas, B. Carroll and L. Cattafesta (2003). Interaction of adjacent synthetic jets in an airfoil separation control application. *33rd AIAA Fluid dynamics Conference and Exhibit* 3709.

Margalit, S., D. Greenblatt, A. Seifert and I. Wygnans (2005). Delta wing stall and roll control using segmented piezoelectric fluidic actuators. *Journal of Aircraft* 42(3), 698-709.

Neuburger, D. and I. Wygnanski (1988). The use of a vibrating ribbon to delay separation on two-dimensional airfoils: some preliminary observations. *Proceedings in Workshop II on Unsteady Separated Flow* 333-341.

Torres, A. J. C. (2017). Flow structure modification

using plasma actuation for enhanced UAV flight control. *Advanced UAV Aerodynamics, Flight Stability and Control: Novel Concepts, Theory and Applications* 547-576.

Wang, J. and J. Wu (2020). Aerodynamic performance improvement of a pitching airfoil via a synthetic jet. *European Journal of Mechanics-B/Fluids* 83, 73-85.

Wang, L., Z. B. Luo, Z. X. Xia, B. Liu and X. Deng (2012). Review of actuators for highspeed active flow control. *Science China Technological Sciences* 55(8), 2225-2240.

Wang, X., J. Yan, J. S Dhupia and X. Zhu (2020). Active Flow Control Based on Plasma Synthetic Jet for Flapless Aircraft. *IEEE Access* 9, 24305-24313

Zhang, W. and R. Samtaney (2015). A direct numerical simulation investigation of the synthetic jet frequency effects on separation control of low-Re flow past an airfoil. *Physics of Fluids* 27(5), 055101-.

Zhang, X., Y. Huang, P. Yang, P. Zhang and Z. Huang (2018). Flight test of flow separation control using plasma UAV. *Acta Aeronauticaet Astronautica Sinica* (2), 121587-1-121587-8.

Zheng, X., X. Zhou and S. Zhou (2005). Investigation on a type of flow control to weaken unsteady separated flows by unsteady excitation in axial flow compressors. *Journal of Turbomachinery* 127(3), 323-330.